297

PRACTICAL ASPECTS OF THE DETECTION AND LOCATION OF PARTIAL DISCHARGES IN POWER CABLES

Task Force D1.02.05

June 2006

cigré

PRACTICAL ASPECTS OF THE DETECTION AND LOCATION OF PARTIAL DISCHARGES IN POWER CABLES

Task Force
D1.02.05

E. Lemke, E. Gulski, W. Hauschild, R. Malewski,
P. Mohaupt, M. Muhr, J. Rickmann, T. Strehl,
F.J. Wester

Content

Abstract:

For enhancement of the reliable operation of power cables network preventive PD diagnosis tests are increasingly performed. In order to assess the insulation condition on the basis of the obtained data, fundamental knowledge on the PD occurrence is required. The presented brochure deals with both, theoretical analysis and experimental studies on the wave propagation of PD pulses in power cables. Furthermore, practical aspects of the detection and location of PD faults are discussed.

Index Terms:
Power cables, travelling waves, partial discharges (PD), PD diagnostics, PD fault location, PD mapping

1. Introduction

The conventional PD measuring method specified in the relevant IEC standards [1; 2] has well been proven under laboratory condition. Presently, this technique is increasingly used under on-site condition, in particular for PD testing of installed power cables [3]. One issue of this paper is to develop an approach which can simply be handled for assessing the sensitivity, which can be achieved for the detection and location of PD defects in long power cables under on-site condition [4]. Furthermore, the PD occurrence is discussed from a practical point of view, such as the impact of the superposition of PD pulses as well as the different wave propagation velocities in mixed cable sections on the location uncertainty [5]. For better understanding first some fundamentals of the very complex PD occurrence in power cables will be presented.

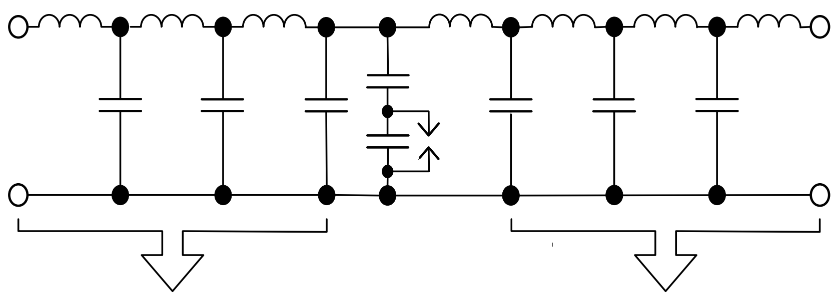

Fig. 1: Equivalent circuit for PD defects in power cables

2. Fundamentals

2.1 PD occurrence in power cables

As known from the literature, partial discharges (PD) are caused by insulation imperfections and bridge only a part of the insulation between the electrodes [6, 7]. Generally it can be distinguished between internal discharges, surface discharges and external corona discharges. The occurrence of internal discharges, which may appear in gas-filled voids, cavities and cracks, is usually explained by the a-b-c model, where the test object is substituted by a lumped capacitor. In geometrically extended test objects, such as power cables, power transformers and rotating machines, the PD pulses propagate like travelling waves. Under this condition the classical a-b-c approach has to be modified accordingly, as evident from Fig. 1. Here the insulation defect is also represented by the capacitor C_c connected in series with C_b which represents the remaining healthy insulation, but the lumped capacitor must be substituted by the characteristic impedance Z_0. If the resulting voltage across C_c becomes higher than the breakdown voltage of the defect, i.e. a puncture of the parallel connected spark gap S_g occurs, a current pulse of extremely short duration, usually in the ns-range, is ignited. For such

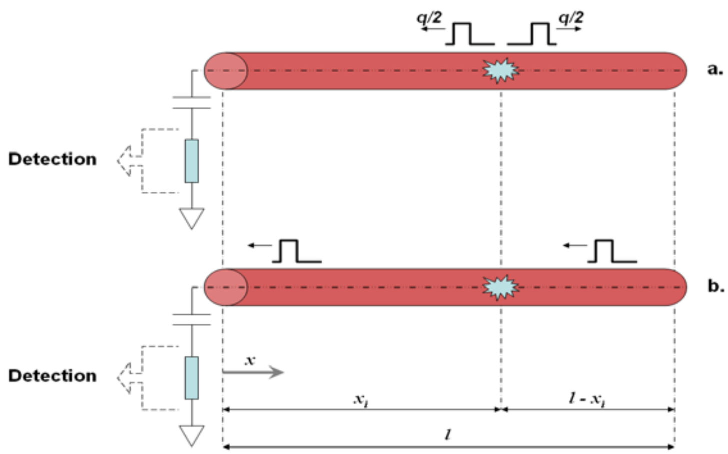

Fig. 2: Principle of PD pulse propagation in power cables
a) just after PD ignition, both pulses travel in the opposite direction
b) after reflection at the "remote end", both pulses travel in the same direction

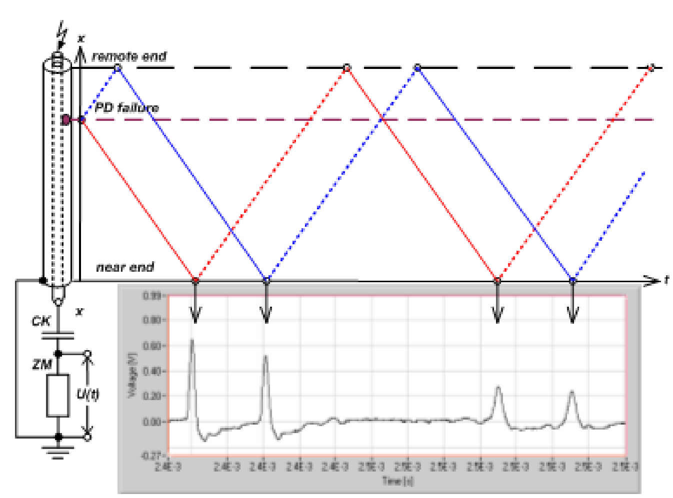

Fig. 3: Principle of the PD fault location using the time domain reflectometry, cable length 1705 m, PD site from near end 1297 m

short pulses long power cables behaves like a travelling wave guide and can therefore not be treated as a lumped capacitor C_a, but by the characteristic impedance Z_0, as mentioned previous. Due to the symmetrical configuration of power cables each PD event produces two equal current pulses, i.e. the pulse charge magnitude $q / 2$ travels away from the PD source in both directions, as schematically reflected in Fig. 2. At the "remote end" of the cable section, which is generally open during the PD measurement, a full reflection occurs. Therefore at the "near end" of the cable, where the PD coupling unit is connected, not only the direct pulse but also the reflected pulse can be detected. This occurrence is used for location the PD site using the time domain reflectometry (TDR), as known from the relevant literature, as for instance [3; 4; 5; 8; 9] and schematically shown in Fig. 3.

Inductance per unit length:

$$L' = (\mu_0 / 2\pi) * [\ln (d_2 / d_1)] \qquad (1)$$

Capacitance per unit length:

$$C' = 2\pi * \varepsilon_0 * \varepsilon_r / [\ln (d_2 / d_1)] \qquad (2)$$

Here are:

- d_1 - the diameter of the inner cable conductor
- d_2 - the diameter of the outer cable conductor
- μ_0 - the permeability constant
- ε_0 - the permittivity constant
- ε_r - the relative permittivity of the extruded cable insulation.

Resistance per unit length due to the skin-effect:

$$R' = [k_c / (\pi * d_1)] * [\omega * \mu_0 / (2 * \kappa_c)]^{1/2} \qquad (3)$$

Here are:

- Ω -the radian frequency $(\omega = 2\pi f)$
- κ_c -the specific conductance of the inner cable conductor
- k_c -a correction factor taking into account the losses in the outer conductor

Conductance per unit length due to the semiconducting layer:

$$G' = [k_s * 4\pi * d_s / (d_1 * \kappa s)] * \{\varepsilon_0 * \varepsilon_r * \omega / [\ln (d_2 / d_1)]\}^2 \qquad (4)$$

Here are:

- κ_s - the specific conductance of the inner semiconducting layer
- d_s - the thickness of the inner semiconducting layer
- k_s - a correction factor taking into account losses in the outer semiconducting layer

Characteristic cable impedance:

$$Z_c = [R' + j\omega L']^{1/2} * [G' + j\omega C']^{-1/2} \qquad (5)$$

Propagation constant:

$$\gamma = [(R' + j\omega L') * (G' + j\omega C')]^{1/2} \qquad (6a)$$

$$\gamma = \alpha + j\beta \qquad (6b)$$

Attenuation constant:

$$\alpha = \Big\{(1/2) * \omega L' * j\omega C' * \{\{[1 + (R' / \omega L')^2] * [1 + (G' / \omega C')^2]\}^{1/2} - 1\} + (1/2) * R' * G'\Big\}^{1/2} \qquad (7)$$

Phase constant:

$$\beta = \Big\{(1/2) * \omega L' * j\omega C' * \{\{[1 + (R' / \omega L')^2] * [1 + (G' / \omega C')^2]\}^{1/2} + 1\} - (1/2) * R' * G'\Big\}^{1/2} \qquad (8)$$

Table 1: Basic equations for analysis of travelling waves in single core power cables

2.2 Attenuation and dispersion of PD pulses in power cables

For the analysis of the PD pulse propagation in long power cables, the travelling wave theory must be used. This is based on the electrical line model, already published at the beginning of the last century [10; 11]. The equivalent circuit is reported in Fig. 4a, where the circuit elements L', C', R' and G' represent the inductance, capacitance, resistance and conductance per unit length, respectively. Taking into account the greater-

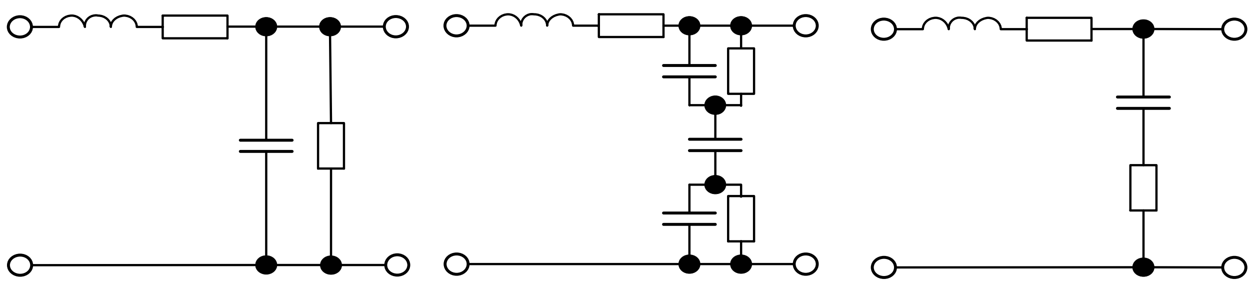

a) **b)** **c)**

Fig. 4: Equivalent networks for analysing the travelling wave occurrence in power cables
a) classical circuit line model **b) complex radial semicon layer loss model [12]**
c) simplified semicon layer loss model

than-expected losses in power cables the radial semiconducting loss model shown in Fig 4b was proposed by Stone and Boggs [12]. Here the circuit elements G_1', G_2', C_1' and C_2' represent the conductance and the capacitance per unit length of the inner and outer semiconducting layer, respectively. This approach has well been proven for frequencies up to 100 MHz and even higher [12]. For the detection and location of PD events in long power cables, however, only frequency modes below 10 MHz are of interest [3]. Thus the very complex circuit shown in Fig. 4b can essentially be simplified as reflected in Fig. 4c. Here R_c' represents the equivalent resistance per unit length of the inner and outer cable conductor, Cs' the capacitance per unit length of the cable insulation and R_s' the equivalent resistance per unit length caused by the inner and outer semiconducting layer. The impact of the parallel capacitances C_1' and C_2' reflected in Fig. 4b can be neglected for frequencies below 10 MHz.

As known from the electrical network theory, the series connection of C_s' and R_s' in Fig. 4c is substitutable by a parallel circuit, composed by the elements C' and G', which is in principle equivalent to Fig. 4a. Consequently, for further considerations the classical electric line model is also applicable for power cables if the characteristic elements R' and G' are modified accordingly, as will be reported more in detail below.

For a single core cable the previous mentioned elements L', C', R' and G' are given by the well known formulas (1) to (4) listed in Tab. 1. For further estimations the basic equations, required for analyzing of travelling waves [10, 11], are also

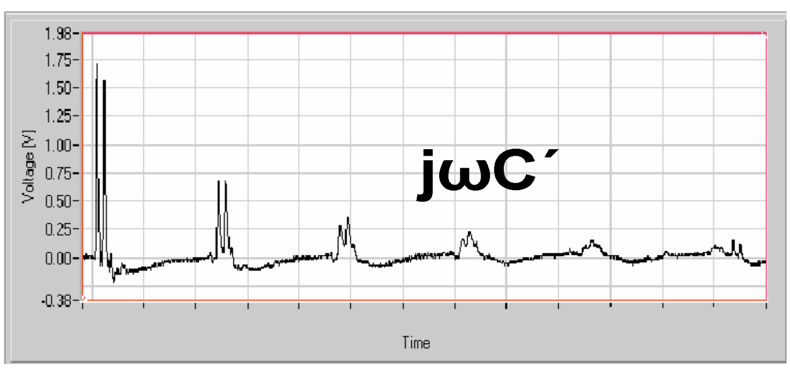

Fig. 5: Attenuation of a multiple reflected PD pulse in a power cable, time base 2.5 µs/div.

listed in Tab. 1 and additionally in Tab. 2. Without going into details it shall be recalled, that travelling waves can generally be considered as the superposition of a forward and a backward propagating wave, given by formula (12) in Tab. 2. For the measurement and location of PD events in power cables usually the forward travelling voltage wave is of interest. Reflecting formula (6b) which can also be expressed by formula (13), the forward propagating PD pulse is given by equation (14). Here the first right term reflects the attenuation of the PD pulse magnitude and the second term the dispersion. For loss-free cables, where the condition (15) is fulfilled, the second right term of equation (14) becomes the value 1. This means that the PD pulse magnitude is attenuated exponentially with the travelling distance, as reflected by the formula (16).

Phase constant of loss-free cables:

$$\beta = \omega\,(L' * C')^{1/2} \qquad (9)$$

Phase velocity:

$$v_p = \omega / \beta \qquad (10)$$

Phase velocity of loss-free cables:

$$v_0 = (L' * C')^{-1/2} = (\mu_0 * \varepsilon_0 * \varepsilon_r)^{-1/2} = c_0 * (\varepsilon_r)^{-1/2} \qquad (11)$$

Voltage wave dependent on the travelling distance:

$$U_w = U_1 * \exp(-\gamma x) + U_2 * \exp(\gamma x) \qquad (12)$$

$$\exp(-\gamma x) = \exp(-\alpha x) * \exp(-j\beta x) \qquad (13)$$

Forward travelling voltage wave of a PD pulse:

$$U_{pd} * \exp(j\omega t) = u_1 * \exp(-\alpha x) * \exp(j\omega t - j\beta x) \qquad (14)$$

Loss-free cables:

$$j\omega t - j\beta x = 0 \quad \rightarrow \omega / \beta = x / t = v_0 \qquad (15)$$

$$U_{pd} * \exp(j\omega t) = u_1 * \exp(-\alpha x) \qquad (16)$$

Table 2: Equations for analysis of PD pulses travelling through single core power cables

The increasing attenuation of PD pulses dependent on the propagation distance is well known from practical PD tests of power cables. As an example, Fig. 5 shows a typical PD pulse reflectogram recorded for a XLPE power cable of 480 m length, where the PD defect occurred at a distance of about 450 m from the near end. Because of the relative high input impedance of the applied PD coupling unit, subsequent pulse sequences occurred, due to multiple reflections at both cable ends. Additionally to the attenuation a dispersion can be observed, i.e. the PD pulse width increases with the travelling distance. This is equivalent to a reduction of the upper frequencies. That means the cable behaves like a low-pass filter. This is also reported in Fig. 6, which reflects the pulse response of a cable sample in the frequency domain [13].

Fig 6a reveals that the injected calibrating pulses are characterized by a frequency spectrum up to about 10 MHz. Because the cable was open at both ends, the arriving pulses are full reflected and traveled

$$v_p = (L' * C' * A_s)^{-1/2} = c_0 * (\varepsilon_r * A_s)^{-1/2} \qquad (17a)$$

$$A_s = [1 + (1 + B_s)^{1/2}] / [2 * (1 + B_s)] \qquad (17b)$$

$$B_s = (\omega\, C_s' * R_s')^2 \qquad (17c)$$

$$E_s = [\ln (d_2 / d_1)] / [\ln [(d_2 - 2d_s) / (d_1 + 2d_s)] \qquad (18)$$

$$v_p = (L' * C' * E_s)^{-1/2} = c_0 * (\varepsilon_r * E_s)^{-1/2} \qquad (19)$$

$$v_p = c_0 * (\varepsilon_r * R_s)^{-1/2} = c_0 * (2.4 * 1{,}35)^{-1/2} = 167\ m/\mu s \qquad (20)$$

Tab. 3: Equations for evaluation the travelling wave velocity

thus several times through the cable. As evident from Fig. 6b the frequency spectrum is significantly reduced, if pulses travelling twice through the cable. This becomes more pronounced after travelling four times (Fig. 6c) and at least six times through the cable (Fig. 6d). Finally only frequencies below 2 MHz remained. This confirms the before mentioned low-pass characteristic of the cable, which is not only caused by the attenuation but also by the dispersion, due to the frequency dependent phase velocity.
That means, in real power cables each frequency mode travels at a specific velocity, as reflected by equation (8). Consequently, the PD pulse width is extended as exemplarily reported in Fig. 7.

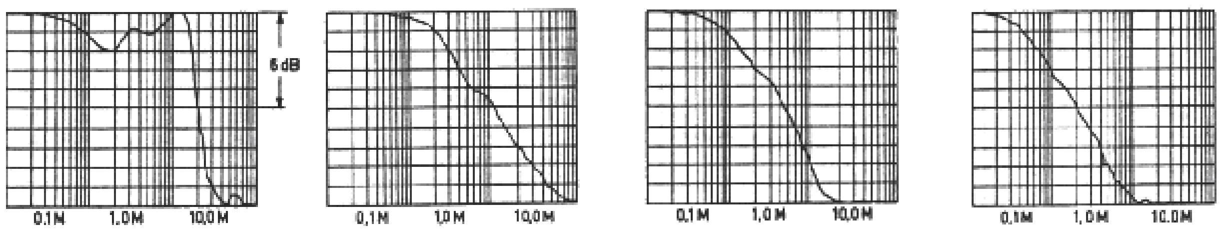

a) b) c) d)

Fig. 6: Frequency spectrum of pulses travelling several times through a power cable
a) direct injected pulse b) after twice the cable length
c) after four times the cable length d) after six times the cable length

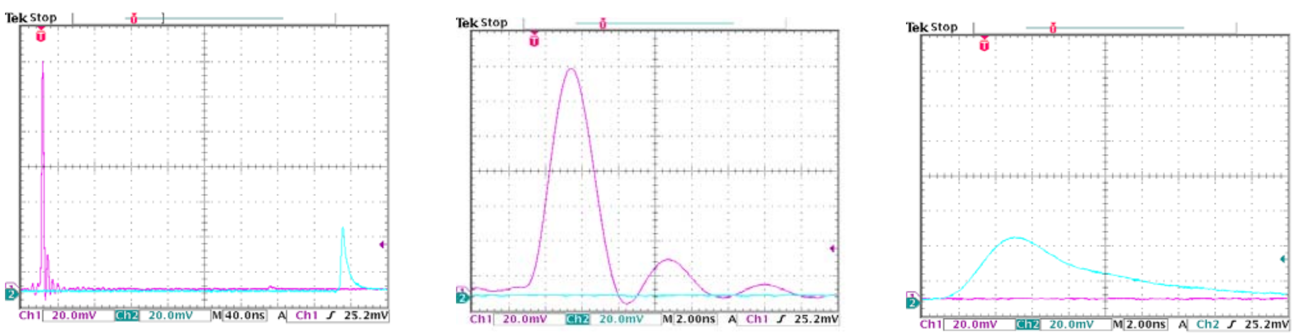

a) b) c)

Fig. 7: Dispersion of a PD pulse travelling through a 52 m long XLPE cable
a) Pulse shape at the near end (left) and remote end (right), time scale 40 ns/div
b) Pulse shape at the near end, time scale 2 ns/div
c) Pulse shape at the far end, time scale 2 ns/div

These records refer to a PD pulse charge magnitude of about 9 pC occurring at one end of a 52 m long XLPE cable sample. After a travel time of 320 ns the PD pulse appeared at the remote end, as can be seen from the right pulse in Fig. 7a, which is equivalent to a wave velocity of 162 m/µs. Whereas the origin PD pulse decoupled from the near end is characterized by a pulse width of only 4 ns (Fig 7b), the PD pulse width measured at the remote cable end is nearly 20 ns (Fig. 7c), which is around 5-times longer if compared to the initial value. Additionally the peak value is reduced substantially, i.e. from originally 130 mV down to about 40 mV, which is less than 30% of the initial value.

2.3 PD wave velocity in XLPE power cables

For location of PD sites the wave velocity v_p is the most important parameter and should thus well be known. For a theoretical analysis of v_p the very complex equations (7) and (8) can strongly be simplified if only frequency modes below 10 MHz are of interest. A useful approximation is given by equation (17a). Because the factor A_s expressed by (17b) is always greater than 1, even if the factor B_s given by (17c) becomes extremely low, it could be written: $v_p > c_0 * (\varepsilon_r)^{-1/2}$. But this relation contradicts the reality, because the velocity of loss-free XLPE cables amounts about 190 m/µs if calculated according to equation (11) for an assumed relative permittivity of $\varepsilon_r = 2.4$. For real XLPE power cables, however, the characteristic values range around 160 m/µs, which is nearly 20% below the theoretically expected value. The main reason for this discrepancy seems to be a fictive enhancement of the capacitance per unit length due to the reduction of the effective insulation thickness between the inner and outer semiconducting layer. In order to verify this assumption the wave velocity of a 24 kV XLPE cable could roughly be estimated on the basis of the following measured parameters:

Relative permittivity of the insulation:	$\varepsilon_r = 2.4$
Diameter of the inner conductor:	$d_1 = 14$ mm
Diameter of the outer conductor:	$d_2 = 27$ mm
Thickness of the semiconducting layers:	$d_s = 0.8$ mm

The characteristic capacitance ratio E_s can be expressed by equation (18) where equation (11) is substituted by the equations (19) and (20) in order to get the phase velocity in the presence of the inner and outer semiconducting layers. Inserting the previous reported cable parameters in formula (20) the velocity becomes 167 m/µs, which is well comparable to the measured velocity of the here considered cable sample, which was 164 m/µs.
In this context it should be mentioned that the very complex occurrence of the PD pulse propagation in shielded power cables has been investigated comprehensively in the past. Exemplarily the references [12 -19] should be mentioned. The published results, however, refer mainly to the frequency domain and not to the time domain, which is required for an evaluation of the attenuation of the PD pulse magnitudes in order to assess the PD detection sensitivity, which can be achieved in very long power cables. Thus, experimental studies on the PD pulse attenuation in power cables were performed in the time domain [4]. In the following some results will be reported more in detail.

3. Experimental studies for evaluating the PD pulse attenuation

3.1 Test procedure

The experiments were performed on power cables of current production. Injecting artificial PD pulses by means of a PD calibrator the pulse response was recorded by a digital scope. Because both, the output impedance of the calibrator and the input impedances of the digital scope, were several orders above the characteristic impedance of the power cables under investigation, the near and remote cable end could be considered as “open”. Consequently, subsequent pulse sequences appeared at the measuring site, due to multiple pulse reflections at both cable ends. As will be shown in the following, this occurrence can be used advantageously for a fictive elongation of the investigated geometrical cable length. This advantage, however, can only be used, if no losses are caused by each reflection. In order to verify this requirement the following check has been performed:

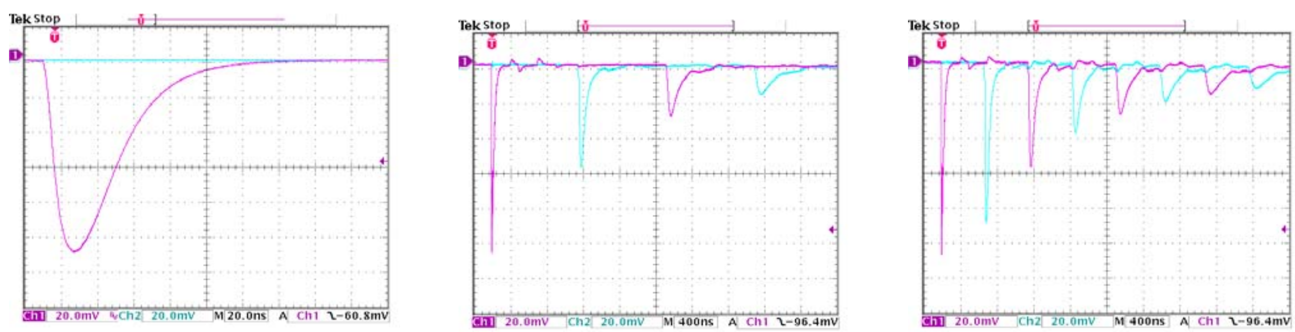

a) **b)** **c)**

Fig. 8: Results of studies on the impact of pulse reflections on the attenuation and dispersion
a) Shape of the injected calibrating pulse, time scale 20 ns/div
b) Reflectogram for a x m long BNC cable, time scale 400 ns/div
c) Reflectogram for a y m long BNC cable, time scale 400 ns/div

First calibrating pulses shown in Fig. 8a were injected in a 200 m long measuring cable and the occurring pulse sequences at both cable ends were recorded by a digital scope (Fig. 8b). After that the cable length was reduced to 50 % of the previous one, i.e. down to 100 m. Consequently, the number of the recorded pulses at the same sweep is increased by twice times (Fig. 8c). For comparison purposes let us first consider the third pulse shown in the record of Fig. 8c, which is caused by the first reflection at the remote end but recorded by the first channel connected to the near end, i.e. the total distance traveled by the pulse amounts $2 * 100$ m = 200 m.

Let us now consider the second pulse in Fig. 8b recorded by the second channel of the scope, which refers to the remote cable end. Because the magnitude of the third pulse in Fig. 8c is equal to those of the second one in Fig. 8b it can be concluded, that no additional attenuation is caused by the reflection. This behavior is also confirmed if the magnitudes of the fifth and of the seventh pulse in Fig. 8c are compared with those of the third and fourth pulse shown in Fig. 8b, respectively. Consequently, an impact of multiple pulse reflections on an additional attenuation of the pulse magnitudes can be excluded.

For a quantitative assessment of the PD pulse attenuation also the following aspect has to be taken into consideration. As known from the travelling wave theory for loss-free cables the second PD pulse due to the reflection at the remote end appears at a higher magnitude compared to the first injected pulse. This can also be observed for short cable lengths, where the losses are comparatively low.

A typical example, which refers to a 33 kV XLPE power cable having a length of 45 m, is reported in Fig. 9. The records reveal the higher magnitude of the second pulse in comparison to the first injected pulse. Because the cable losses can not be neglected, the peak value of the second pulse is not twice the magnitude of the first one, as to be expected from a theoretical point of view. Due to this occurrence only the peaks of the reflected pulses were evaluated in order to avoid any misinterpretations of the experimental results. Consequently, the calibrating pulses were injected at the remote end.

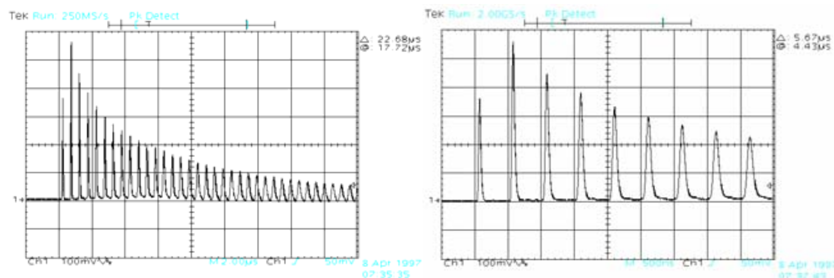

Fig. 9: Characteristic pulse reflectogram obtained for a 30 kV XLPE of 45 m length, recorded at a time scale of 2 µs/div (left) and 0.5 µs/div (right)

Cable-No.	Rated Voltage [kV]	Length [m]	Virtual Length [m]	Wave Velocity [m/µs]
1	24	448	5376	163
2	33	45	1350	162
3	33	486	4860	163
4	33	704	9856	161
5	138	175	2450	168

Table 4: Survey on the investigated power cable samples

As already mentioned, for the detection and location of PD events in power cables only a frequency spectrum below 10 MHz is of interest. Therefore, the results reported in the following refer to a limitation of the upper cut-off frequency down to about 10 MHz, which is equivalent to a step pulse rise time of the complete measuring system of about 30 ns.

3.2. Test results

The experimental investigations were executed on power cables listed in Tab. 4. Here besides the geometrical length also the virtual length is presented, which results from the evaluation of subsequent appearing pulse sequences due to multiple pulse reflections at both open cable ends, as already reported previous.

A typical measuring example is reported in Fig. 10, which

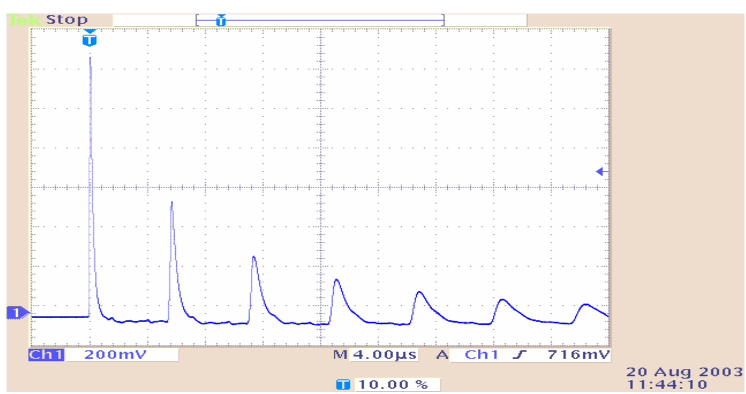

Fig. 10: Time domain reflectogram obtained by injecting of artificial PD pulses in a 448 m long XLPE cable

refers to the cable No. 1. Here the geometrical length was 448 m. Because the characteristic time interval between the subsequent appearing pulses is 5.5 µs, which results from a travelling distance of twice the cable length, the wave velocity amounts 163 m/µs, which is also listed in Tab. 5. In total 7 individual pulses could be evaluated from the recorded reflectogram (see Fig. 10). Therefore the virtual length can be estimated by (7-1) x 2 x 448 m = 5376 m. In accordance to this calculation the virtual lengths of all other investigated cables are also listed in Tab. 4. In order to evaluate the pulse attenuation depend on the travelling time the peaks of the subsequent appearing pulses (see Fig. 10) were analyzed accordingly.

A survey on the experimental gained data is presented in Fig. 11. Here the peak value of the first recorded pulse is used as a reference, i.e. 100 %. With respect to a better resolution this value is not plotted in the graphs.

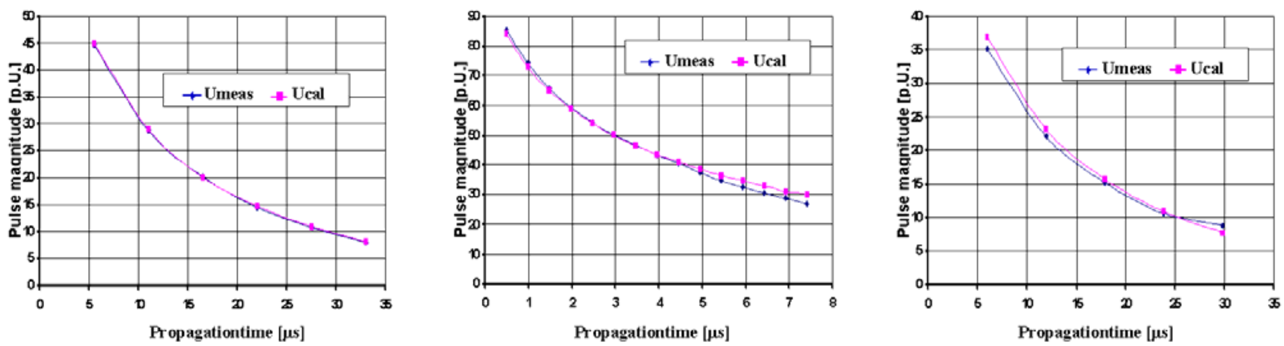

a) Cable 1: T_1 = 5 µs, T_2 = 18 µs b) Cable 2: T_1 = 3 µs, T_2 =15 c) Cable 3: T_1 = 3 µs, T_2 = 18 µs

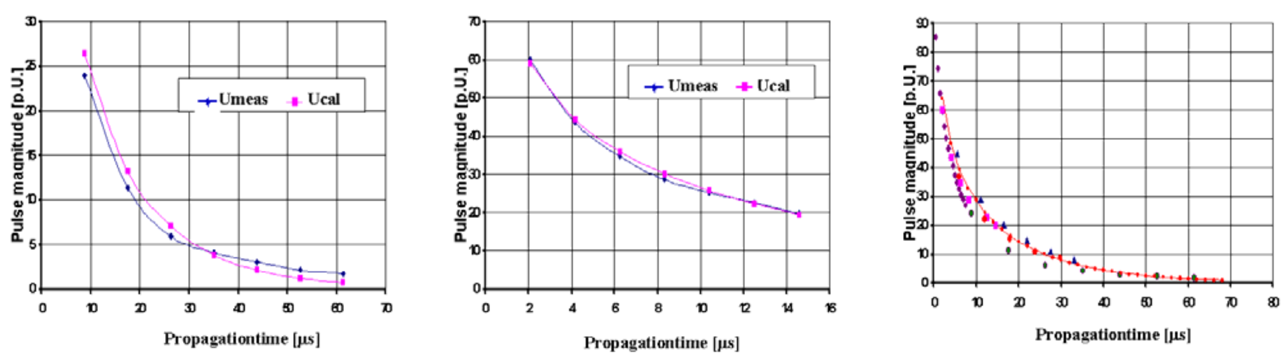

d) Cable 4: T_1 = 3 µs, T_2 = 15 µs ***e) Cable 5: $T_1 = 3\ \mu s$, $T_2 = 15\ \mu s$*** ***f) Cables 1 to 5: $T_1 = 4\ \mu s$, $T_2 = 18 \mu s$***

Fig. 11 reveals that the measured data can well be fitted by an empirical approach, which is given by equation (21). For comparison purposes additionally to the measured data also the calculated curves using equation (21) are plotted in the graphs, displayed in Fig. 11a to 11e. Additionally, in Fig. 11f all measured data are plotted together with a mean curve calculated by (21) using the characteristic time parameters $T_1 = 4\ \mu s$ and $T_2 = 18\ \mu s$. This graph reveals that equation (21) works quite well. Thus approach (21) is used in connection with the characteristic time parameters for further analysis, where the travelling time t is substituted in accordance to formula (22) by the travelling distance x. Here the velocity v_p is approximated by a mean value of 160 m/µs. Under this condition the time constants T_1 and T_2 can be expressed by equivalent lengths, as evident from the equations (23a) and (23b). Recalling equation (16) the PD pulse attenuation dependent on the travelling distance is also given by equation (25). Because the attenuation in power cables is generally expressed in dB/m or in dB/km, the equation (24b) shall be expressed accordingly, using equation (26).

$$U_t = U_0 * \exp[(-t/T_2) - t/(t+T_1)] \qquad (21)$$

U_t - the pulse magnitude appearing after the travelling time t
U_0 - the peak value of the first pulse, i.e. the 100 % reference value
T_1 - a first time constant, ranging between 3 µs and 5 µs.
T_2 - a second time constant, ranging between 15 and 20 µs.

$$t = x / v_p \;;\; x = t * v_p \qquad (22)$$

$$T_1 = X_1 / v_p ;\; X_1 = T_1 * v_p = 4\,\mu s * 160\,m/\mu s = 0.64\,km \qquad (23a)$$

$$T_2 = X_2 / v_p ;\; X_2 = T_2 * v_p = 18\,\mu s * 160\,m/\mu s = 2.88\,km \qquad (23b)$$

$$U_x = U_0 * \exp[(-x/X_2) - x/(x+X_1)] \qquad (24a)$$

$$U_x = U_0 * \exp[(-x/2.88\,km) - x/(x+0.64\,km)] \qquad (24b)$$

Tab. 5: Equations for evaluation the PD pulse attention in extruded power cables (I)

In order to evaluate the frequency dependent attenuation equation (7) can be simplified, if only frequencies below 10 MHz are taken into consideration. Under this condition the equations (27a) and (27b) are generally fulfilled. Thus the attenuation constant reflected by equation (7) can be approximated by (28a). After inserting the equations (3) and (4) we get the equation (28b).

Here are:

$d_3 = d_1 + 2\, d_s$

$d_4 = d_2 - 2\, d_s$

k_{cs} - a correction factor,

which takes into account the additional losses in both, the outer cable shield as well as in the outer semiconducting layer.

Based on formula (28b) the attenuation α_d in dB/km as function of the frequency $f = \omega/2\pi$ has been calculated for a 24 kV XLPE cable, with the following cable parameters: $d_1 = 14\,mm$, $d_2 = 27\,mm$

$d_s = 0.7\,mm$, $\varepsilon_r = 2.4$

$\kappa_c = 3.54 * 10^7\,S/m$

$\kappa_s = 2 * 10^{-2}\,S/m$, $k_{cs} = 1.7$

$$\alpha_x = (1/2.88\,km) + 1/(x + 0.64\,km) \qquad (25)$$

$$\alpha_d = 20 \log (U_x / U_0) = 8.686 * \alpha_x$$
$$= 8.686 * [(1/2.88\,km) + 1/(x + 0.64\,km)] \qquad (26)$$

$$R'/j\omega L' << 1 \quad G'/j\omega C' << 1 \qquad (27a)$$

$$\{[1 + (R'/\omega L')^2] * [1 + (G'/\omega C')^2]\}^{1/2} - 1 = 0 \qquad (27b)$$

$$\alpha_d = (R' * G'/2)^{-1/2} \qquad (28a)$$

$$\alpha_d = k_{cs} * \Big\{(2d_s/\kappa s) * [\mu_0 / (2 * \kappa_c)]^{1/2} * \{\varepsilon_0 * \varepsilon_r / [d_1 * \ln(d_4/d_3)]\}^2 \Big\}^{1/2} * \omega^{5/4} \qquad (28b)$$

$$\alpha_d = (\alpha_{d10} / f_0) * f_m = (2.125\,dB/km) * f_m \qquad (29a)$$

$$\alpha_{d2} = (\alpha_{d20} / f_0) * f_m = (2.375\,dB/km) * f_m \qquad (29b)$$

Tab. 6: Equations for evaluation the PD pulse attention in extruded power cables

The obtained graph is displayed in Fig. 12 and indicated by *"C03"*. It seems of interest, that this calculated curve is quite well covered by the approach of Stone and Boggs [12] derived from the radial semiconductive loss model (see Fig. 4b). For a 28 kV XLPE cable they calculated for a frequency of 80 MHz an attenuation of $\alpha_{d10} = 0.17\ dB/m$ and measured a value of $\alpha_{d20} = 0.19\ dB/m$. Furthermore they found that the attenuation dependent on the measuring frequency can roughly be approximated by a linear function, given by the equations (29a) and (29b). The curves calculated from these relations are indicated in Fig. 12 by *"C01"* and *"C02"*.

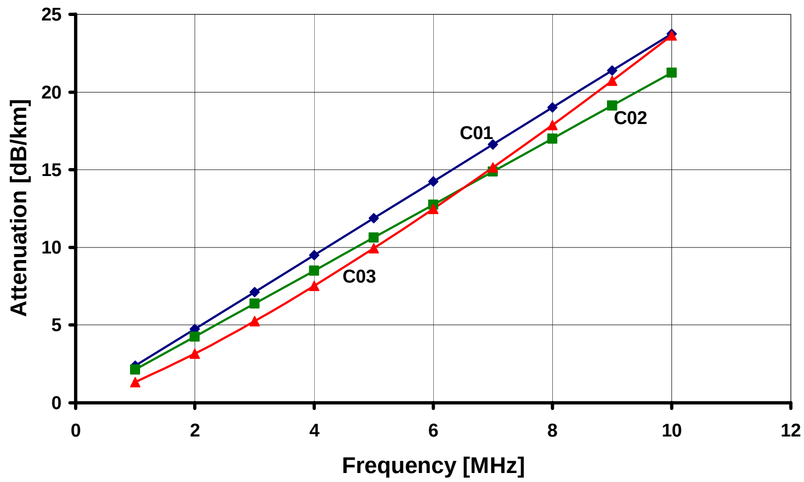

Fig. 12: Calculated attenuation of travelling waves in XLPE cables dependent on the frequency
C01- equation (29a); C02 - equation (29b); C03 - equation (28b)

Based on the here obtained results it can be concluded, that the approach according to equation (28b) is in principle applicable for a quantitative assessment of the attenuation in power cables. In this context it has to be stressed, that this approach refers only to the frequency domain and not to the time domain, but only the latter ensures an estimation of the attenuation of the PD pulse magnitude as function of the travelling distance in order to evaluate the PD detection sensitivity for very long MV power cables. Thus the better approach is equation (26) as will be reported now more in detail.

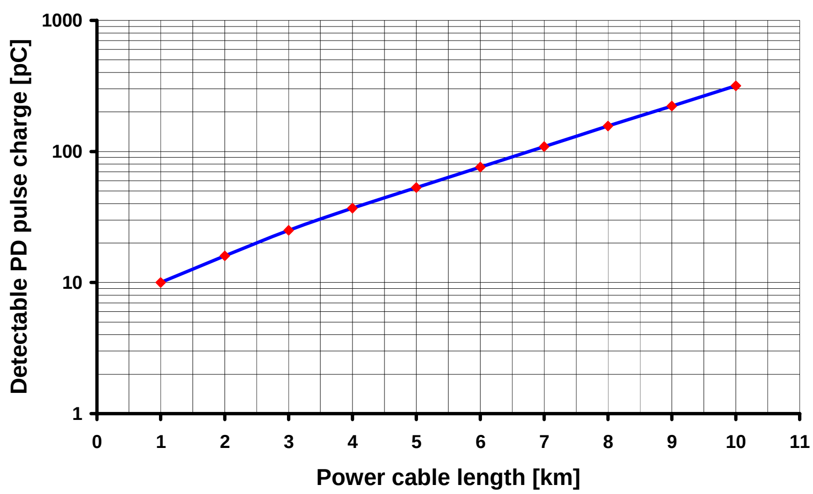

Fig. 13: PD detection sensitivity dependent on the cable length calculated on the basis of a reference value of 10 pC achievable for a power cable of 1 km length

Taking into account the background noise level under on-site condition, the worst case arises, if the PD source is located at the remote cable end, for which the travelling distance x of PD pulses is equal to the whole cable length x_c. PD events can only be recognized if the peak value of the PD pulses, which arrive at the near cable end, exceed significantly the ambient noise level U_n. Recalling equation (24b) the condition (30) must be fulfilled. Because the cable acts as a low-pass filter, as already mentioned previous, a quasi-integration of the propagating pulses takes place. Therefore, after longer travelling distance, say $x_c > 1\ km$, the peak value appearing at the near cable end can be considered as a measure for the apparent charge. Thus equation (30) can also be expressed by equation (31).

For better understanding let us first consider a power cable having a length of $x_c = 1\ km$ as a reference. Additionally, an apparent charge of q_{min} = 10 pC, produced by a PD source at the remote end, should be detectable using a PD measuring circuit in compliance to the relevant IEC standards [1; 2]. Reflecting equations (27 a) and (27 b) we get from equation (32) that the origin PD magnitude of 10 pC is attenuated at the near end down to an equivalent magnitude of $q_{meas} = 3.8\ pC$. This value can only be detected, if the ambient noise level is significantly lower. Assuming that the ambient noise level will not change, if power cables longer than 1 km are tested, the formula (33) applies. Based on these assumptions the minimum detectable apparent charge q_{min} as function of the cable length x_c has been calculated and plotted in Fig. 13. This graph reveals that PD events below 100 pC could never be detected for cable lengths above 7 km. For cable lengths above 10 km the critical PD threshold level exceeds 300 pC.

$$U_0 * \exp[(-x_c/2.88\ km) - x_c/(x_c + 0.64\ km)] > U_n \qquad (30)$$

$$q_{min} * \exp[(-x_c/2.88\ km - x_c/(x_c + 0.64\ km)] > q_n \qquad (31)$$

$$q_n < (10\ pC) * \exp[(-1) * (1/2.88 + 1/1.64)] = 3.8\ pC \qquad (32)$$

$$q_{min} = (3.84\ pC) * \exp[(x_c/2.88\ km) + x_c/(x_c + 0.64\ km)] \qquad (33)$$

Here are:

q_{min} - the apparent charge created by a PD source located at the remote cable end ($x = x_c$)

q_n - the ambient noise level expressed by an equivalent charge

Tab. 7: Equations for evaluation the PD detection sensitivity

Finally it should be mentioned, that with respect to simplified calculations only a homogenous single core cable was considered. An installed power cable line, however, is generally composed of several cables. Due to different wave impedances of the cable sections and the joints each connecting point causes partial pulse reflections, as exemplarily reported in Fig. 14. This is equivalent to an energy loss and causes thus an enhancement of the PD pulse attenuation compared to a homogenous cable structure.

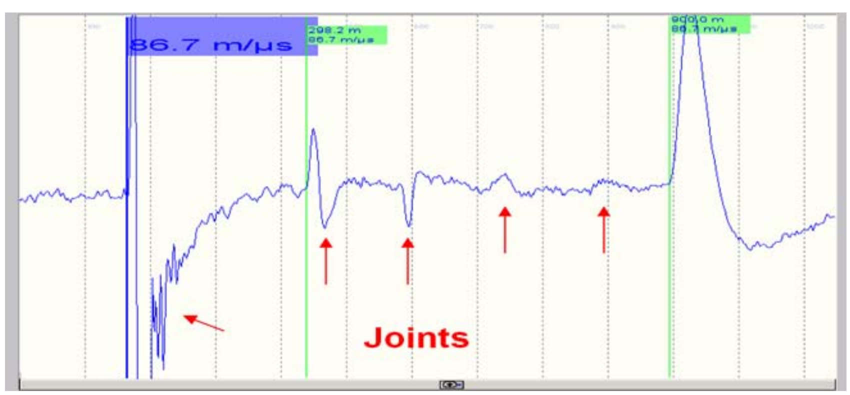

Fig.14: Time domain reflectogram of a power cable showing partial pulse reflections caused by six joints distributed along a power cable section

4. Practical aspects of PD fault location

4.1 Single PD source

If a PD source is active in a power cable line, the occurring pulses will travel away from the PD source towards both cable ends, as already reported in the figures 2 and 3. For location of PD defects generally the time domain reflectometry (TDR) is used. Whereas the direct PD pulse appears at the time t_1, the reflected pulse appears at the time t_2. Therefore the characteristic time difference given by equation (34) can be considered as a measure for the distance of the PD source from the far end, given by equation (35 a).

Based on this relation the PD fault distance from the near end, where the PD pulses are decoupled, can be expressed by equation (35 b).

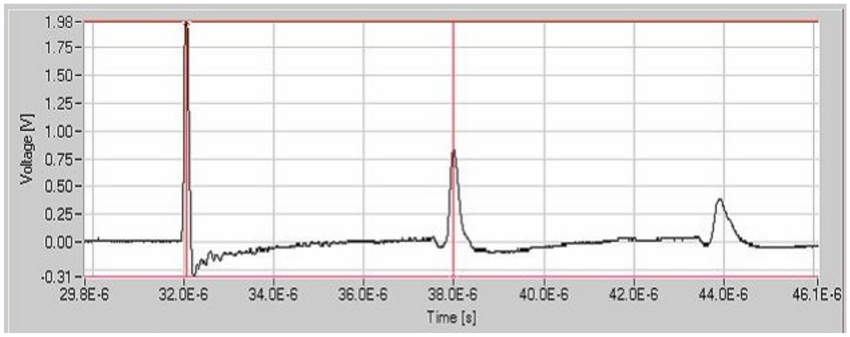

Fig. 15: Practical example for measuring the wave velocity of PD pulses in a XLPE cable

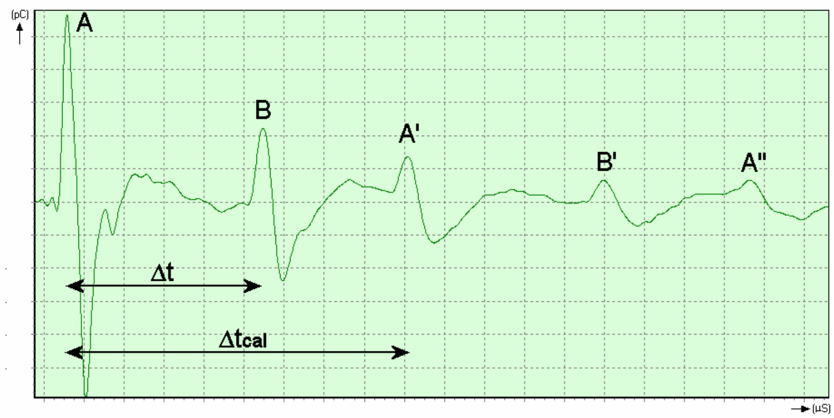

Fig. 16: Location of the PD site in a power cable by evaluation the time difference between the direct pulse (A) and the reflected pulse (B)

Here *l* represents the total power cable length. As evident from this formula, the uncertainty in PD fault location is not only governed by the true determination of the characteristic time difference Δt but also by the true knowledge of both, the propagation velocity v_p and the cable length l.

$\Delta t = t_2 - t_1$	*(34)*
$x_{21} = v_p * \Delta t / 2$	*(35 a)*
$x_{12} = l - (v_p * \Delta t) / 2$	*(35 b)*

Tab. 8: Equations for calculation the PD site

As already mentioned previous, the wave velocity of PD pulses in real power cables is substantially lower as the theoretical one given by equation (11). Therefore, v_p has to be determined experimentally. This is done by the injection of calibrating pulses into one cable end and measuring the time difference between the first (direct) and second (reflected) pulse. A typical time domain reflectogram obtained by the calibration of a 480 m long XLPE cable is reported in Fig. 15. The time difference between the first and second pulse amounts 5.9 µs, thus the propagation velocity can be predicted by the simple relation $v_p = 2 * 480\ m / 5.9\ \mu s = 163\ m/\mu s$.

Figure 16 refers to a practical example of on-site PD location, where the power cable was subjected to a damped AC test voltage [3]. Whereas the first detected pulse (A) arrived direct from the PD source at the near cable end (direct pulse), the second one (B) arrived delayed due to the reflection at the remote cable end (reflected pulse). Because the input impedance of the PD coupling unit exceeds substantially the cable impedance, the direct pulse is also reflected at the detection side and appears hence again (A') after travelling twice through the cable length. From the time difference between the direct (A) and the reflected pulse (B), together with the calibrated propagation velocity, the PD site can simply be calculated by equation (35 b).

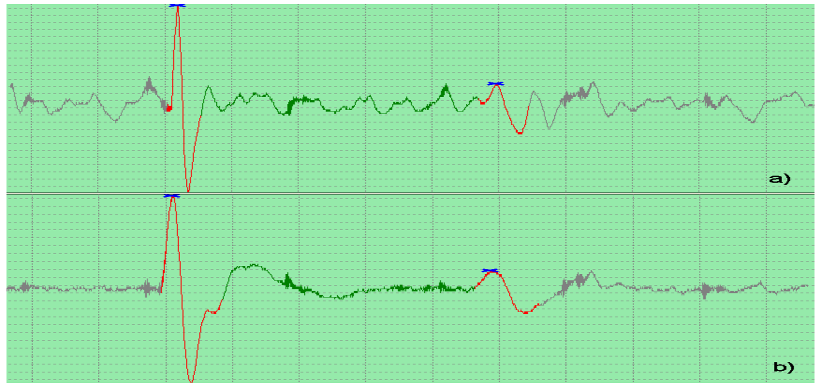

Fig. 17: Time resolved PD pulses obtained from the "near" (upper) and the "remote" termination

In principle it could happen that the time difference between the direct pulse (A) and the reflected pulse (B) is equal to the time difference obtained by the calibration procedure. This special case appears, if the PD´s are located in either the near or the remote cable termination. To determine which of both terminations are affected by PD´s, the analysis of the pulse shape is a useful tool, because the pulse width increases with increasing propagation time, due to the already discussed dispersion. As an example, Fig. 17 reflects a typical record, where the upper trace refers to the termination, where the PD defect is originated and where also the PD coupling unit is connected. The shorter duration of the first (direct) pulse is well visible compared to the pulse from the lower trace, obtained after connecting the PD coupling unit to the opposite cable termination.

Another typical situation might occur by the superposition of the direct and reflected PD pulses, as exemplarily shown in Fig. 18. This will happen if the time interval between the both characteristic pulses is comparable to the duration of the direct pulse. If, for instance, a PD pulse width of 1 µs is measured at the near end, such superposition effects may appear for a critical distance of the PD site from the remote end of less than 80 m due to the characteristic value of $v_p / 2 = 80\ m / \mu s$.

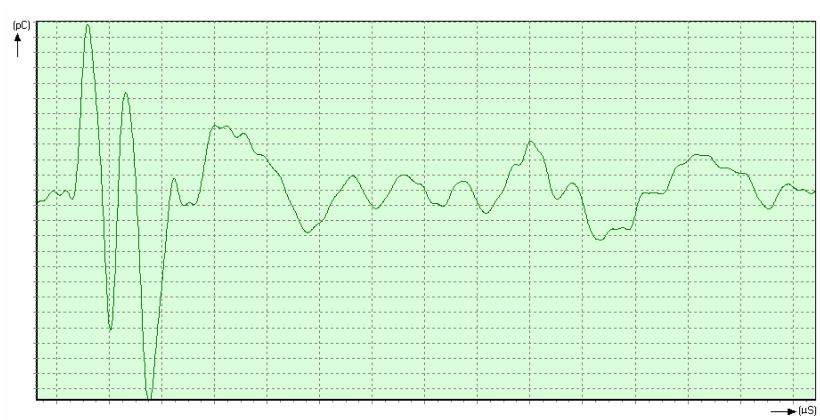

Fig. 18: Superposition of the direct end reflected PD pulse

4.2 Multiple PD sources

During HV energizing of a cable section in the field, several PD sources distributed along the cable can also become active simultaneously. As a result, in just a small time interval, PD pulses can be detected from different locations along the cable length. Although the time differences between the different PD activities may become less than 10µs they are generally still distinguishable because of the comparatively high propagation velocity. A typical example for this is shown in Fig. 19, which refers to three different PD activities originated from two defects, recognized in a 270 m long 3-phase paper insulated cable (PILC). Analyzing the time differences between the direct pulses *(A_i, B_i, C_i)* and the reflected pulses *(A_r, B_r, C_r)* it can be stated, that the PD events *A* and *C* are originated from the same source, whereas *B* is due to another source. Because the received direct pulses travel back and forward again, also the complementary pulse sequences *(Ai', Bi', Ci')* appear in Fig. 19. In this measuring example the relevant time difference of about 2.4 µs is equal for the PD occurrences *A* and *C*. Using equation (35) the distance of the PD source from the remote end can be calculated as 192 m if a mean velocity of $v_p /2 = 80\ m / \mu s$ is assumed.

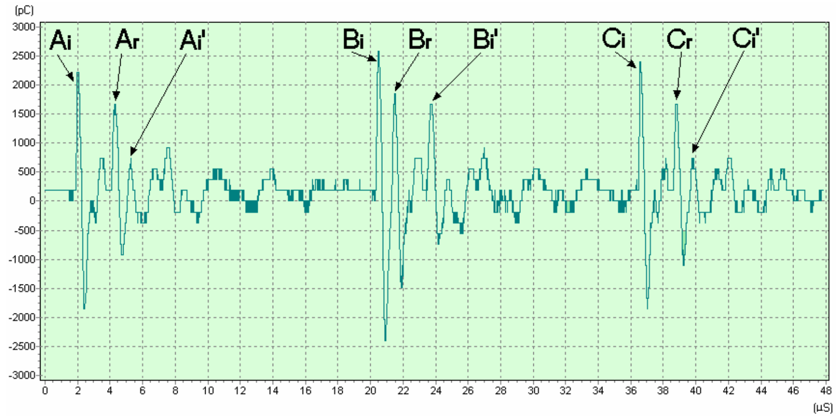

Fig. 19: Multiple PD events occurring during a time span of only 45µs

For the characteristic PD event *B* the time difference is about 1µs. Thus the PD source is located about 80 m from the remote end. That means, in the time interval between the succeeding PD events *A* and *C*, which is about 33 µs, the PD event *B* occurred in another location along the cable.

Partial discharges may also occur, which originate from different defects in the power cable within a time interval less than the characteristic propagation time, as reported in Fig. 20a. The two significant PD events are indicated by *S* and *T*. In the location analysis the direct and the reflected PD pulses are running through each other, where the direct pulse of PD event *T* (T_i) is detected before the reflected pulse of PD event *S* (S_r).

Fig. 20b shows an example obtained for a 610 m PILC section. The indicated PD events *Y* and *Z* are originated from the same defect, because the time differences Δt_Y and Δt_Z between the direct and the reflected pulse are equal. In general the overlapping pulse diagrams for different PD events are dependent on the following three factors:

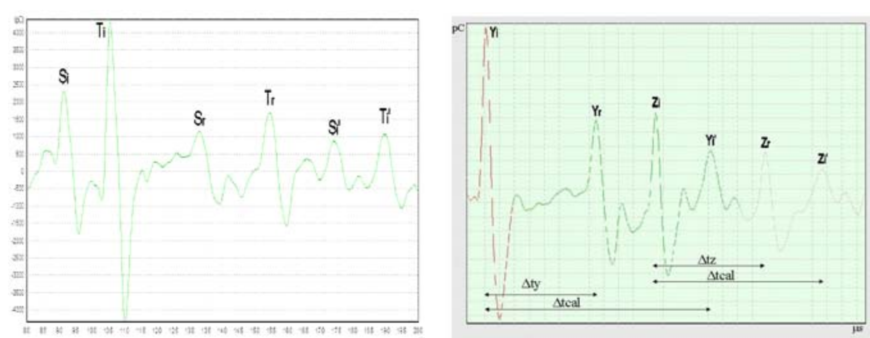

a) **b)**

Fig. 20: Examples for PD location diagrams with overlapping PD pulses from different PD sources (a) and from the same PD source (b)

1. Number of PD defects
2. Length of the power cable
3. Frequency of the test voltage

If the number of defects in a cable sample increases, the number of PD events will naturally increase. The time interval, where the matching PD pulse may occur, is proportional to the length of the cable sample. Thus the probability for overlapping reflectograms will increase for longer power cables.

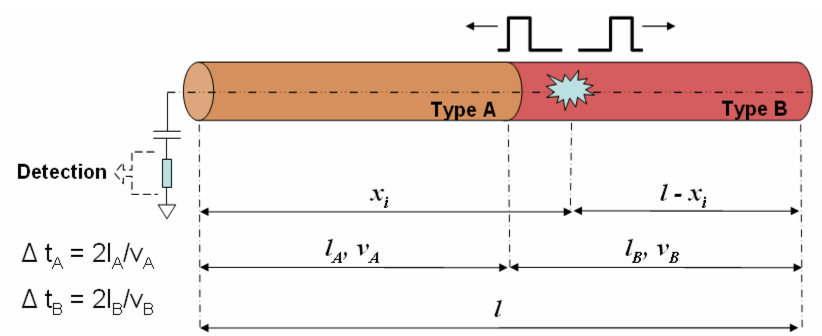

Fig. 21: Schematic view of the propagation of PD pulses in mixed power cable sections

4.3 Mixed cable systems

Due to changes from impregnated paper insulation to plastic insulation for power cables, more and more situations will occur where different insulation types are mixed in cable networks. Because of the different propagation velocities for the different insulation types, errors and misinterpretations may occur in the PD fault location. Fig. 21 shows a schematic view of a mixed cable section, existing of two cable parts of different insulation types A and B, each with a different propagation velocity v_A and v_B , respectively.

$$v_{AB} = 2 * (l_A + l_B) / \Delta t \qquad (36)$$

$$\Delta t = 2 * l_A / v_A + 2 * l_B / v_B \qquad (37)$$

$$v_{AB} = (l_A + l_B) / (l_A / v_A + l_B / v_B) \qquad (38a)$$

$$v_{AB} = (l_A + l_B) * v_A * v_B / (l_A / v_B + l_B / v_A) \qquad (38b)$$

1. $\Delta t_{xi} < \Delta t_{xB}$,
i.e. the PD fault is originated in the part B:

$$x_{iB} = (l_A + l_B) - v_B * \Delta t_{xi} / 2 \qquad (39)$$

2. $\Delta t_{xi} > \Delta t_{xB}$,
i.e. the PD fault is originated in the part A:

$$x_{iA} = l_A - v_A * (\Delta t_{xi} - \Delta t_{xB}) / 2 \qquad (40)$$

Tab. 8: Equations for evaluation the PD site in mixed cables

If a PD occurs at location x_i, the direct and the reflected PD pulse will travel different lengths trough both cable parts. Therefore, another approach for the location of the PD source is necessary than for the single cable type location, reflected by equation (35).
Based on the classical calibration procedure, the wave propagation velocity resulting from the time difference between the direct and reflected pulse can be considered as an "average" velocity of the mixed cable section given in Tab. 8 by the equation (36). The measured time difference Δt depends on the ratio between the lengths of different cable types and their characteristic propagation velocities, as expressed by equation (37). By combination of (36) and (37) we get finally the equations (38 a) and (38b). For analysis of the PD origin locations in mixed cable sections, again the time difference

between the direct and the reflected PD pulse is measured. The next step is, however, to find out from which cable part the PD pulse is coming from. Therefore, the measured time difference Δt_{xi} is compared with the travelling time difference Δt_{xB} to be expected for the cable part B, which is the remote part from the detection side.

For $\Delta t_{xi} < \Delta t_{xB}$ the PD source must be located in the remote cable part B, whereas for $\Delta t_{xi} > \Delta t_{xB}$ the PD source must be originated in the near cable part A. For $\Delta t_{xi} = \Delta t_{xB}$ the PD occurs exactly in the cable joint connecting both cable parts A and B.

As a result, after the distinction from which cable part the PD pulse is originated, the location of the discharge source can be calculated according to the conditions (39) and (40):

Figure 22a reflects a practical measuring example for a possible location error, due to a mixed insulated power cable section. The investigated cable sample was a combination of a XLPE cable having a length of 465 m with a PILC cable of 561 m length. Both PD maps show the individual PD locations along the power cable length for all three phases, where the black dots reflect the accessories.

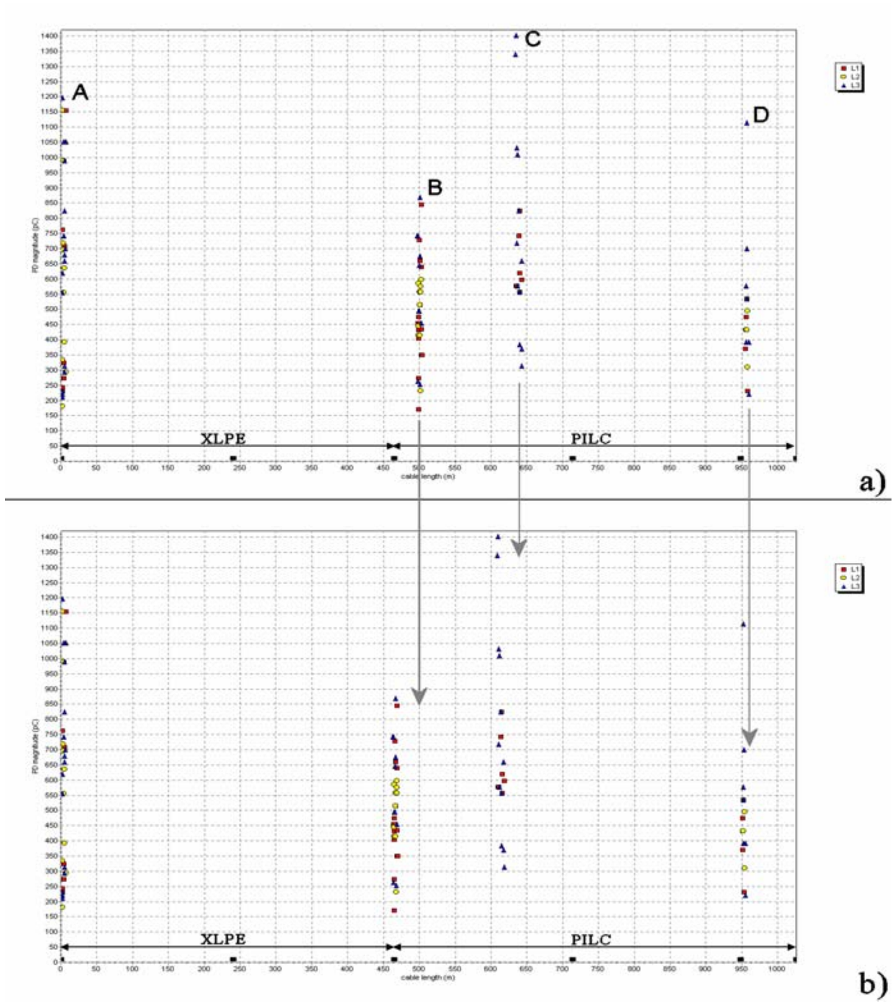

Fig. 22: Practical example for errors in PD mapping of mixed power cables (XLPE + PILC)
a) Using conventional single cable location technique based on equation (35 b)
b) Using modified location technique based on equations (38) to (40)

The upper PD map (a) is created by the conventional location technique valid for non-mixed cables, which reveals four PD concentrations at the locations:

$$A = 0 \text{ m}, \quad B = 500 \text{ m}, \quad C = 645 \text{ m}, \quad D = 955\text{m}$$

If the measured data of the same cable sample are analyzed by means of the equations (38) to (40), where the characteristic velocities v_A = 140 m/µs and v_B = 160 m/µs are used, another PD map is obtained, as reflected in Fig. 22b. The measured PD concentrations are qualitatively well comparable to the plots of Fig. 22a, but the determined PD sites along the cable differ significantly.
As expected, the PD concentration for A = 0 m did not shift, but the other three concentrations shifted as follows:

- B shifted from 500m to 465m, which is 35 m lower
- C shifted from 645m to 620m, which is 25 m lower
- D shifted from 955m to 949m, which is 6 m lower

The here presented practical measuring examples underline the very complex matter of the PD location technique, which is currently increasingly applied for on-site PD testing of MV power cables [4]. In principle also other aspects have to be taken into consideration, such as the already mentioned enhanced PD pulse attenuation due to numerous joints in a cable section, which causes partial pulse reflections. Also a bad condition of the cable shield due to corrosion may contribute to an increased attenuation of the propagating PD pulses, which may essentially reduction the PD detection sensitivity. Such effects have also to be taken into consideration if installed MV power cables are PD tested, but it is not the aim of this paper to present all PD occurrences which may happen under practical conditions.

5. Summary

Based on theoretical analysis and experimental studies of the PD occurrence in long power cables the following conclusions can be drawn:

1. For assessment the attenuation of PD pulses in principle the classical travelling wave theory based on the electric line model is applicable.

2. Because for the measurement and location of partial discharges in MV power cables only a frequency spectrum below 10 MHz is of interest, the radial semiconducting loss model proposed by Stone and Boggs [12] can essentially be simplified.

3. The theoretical analysis can further be simplified if the calculation refers only to the inner semiconducting layer, whereas the impact of the outer semiconducting layer is taking into account by a correction factor, which ensures a comparatively simple estimation of the frequency dependent attenuation and dispersion.

4. It is supposed, that the excessive reduction of the travelling wave velocity below the theoretically expected value is caused by a fictive enhancement of the capacitance per unit length due to a fictive reduction of the insulation thickness by the inner and outer semiconducting layer.

5. The simplified approach has successfully been proven for quantitative assessment of the wave attenuation in the frequency domain. For evaluation of the PD detection sensitivity, however, the analysis must be done in the time domain. In order to get the necessary parameters comprehensive practical studies on the PD wave propagation in long power cables have been performed.

6. Using an instrumentation of comparatively high input impedance the injected pulses were full reflected both, at the near and the far end. Thus results could be obtained for virtual cable lengths much longer than the investigated geometrical cable lengths.

7. Based on experimental data an empirical approach was derived to ensure a simple estimation of the attenuation PD pulses dependent on the travelling distance. This allows an assessment of the PD detection sensitivity, which can be achieved for very long power cables.

8. If on-site PD tests of power cables are executed, besides the attenuation also superposition phenomena of the direct and reflected pulses have to be taken into consideration. This may happen if the PD site is close to the far end as well as if multiple PD sources, distributed along the cable length, ignite simultaneously.

9. The uncertainty in PD location may be enhanced for mixed cable sections because of the different wave propagation velocities in different cable types, such as XLPE and PILC.

6. References

[1] High-voltage test techniques – Partial discharge measurement. IEC 60270 (2000)

[2] Testing of cables, wires and flexible cords – Partial discharge measurement. IEC 60885-3 (1988)

[3] E. Gulski, E. Lemke, M. Gamlin, E. Gockenbach, W. Hauschild, E. Pultrum: Experiences in partial discharge detection of distribution power cable systems. ELECTRA 35 (2003) No. 208

[4] E. Lemke, T. Strehl: Möglichkeiten und Grenzen der TE-Fehlstellenortung in kunststoffisolierten Energiekabeln unter Vor-Ort-Bedingungen. ETG-Fachtagung Köln (2004) pp. 209-213

[5] F.J. Wester, Condition Assessment of Distribution Power Cables using PD Diagnosis at Damped AC Voltages, PhD Thesis TU Delft (2004), ISBN 90-8559-019-1

[6] A. Gemant, W. Philippoff: Die Funkenstrecke mit Vorkondensator. Z. f. Physik 13 (1932) 9, pp. 425-430

[7] F. H. Kreuger: Discharge detection in high-voltage equipment. Temple Press, London (1964)

[8] E. Lemke: A new method for PD measurement of polyethylene insulated power cables. 3rd. ISH Milan (1979) paper 43.13

[9] M. Beyer, W. Kamm, H. Borsi, K. Feser: A new method for detection and location of distributed partial discharges in high voltage cables under external interference.
IEEE Trans. PAS 101 (1982) 9, pp. 3431-3437

[10] L. Binder: Über Einschaltvorgänge und elektrische Wanderwellen. ETZ 35 (1914) pp. 177 and 203

[11] R. Rüdenberg: Elektrische Schaltvorgänge. Springer-Verlag Berlin (1933)

[12] G.C. Stone, S.A. Boggs: Propagation of partial discharge pulses in shielded power cables. Proceedings of Conference on Electrical Insulation and Dielectric Phenomena. IEEE Publication 82CH1773-1(1982) paper V-6, pp. 275-280

[13] P. Osvath, G. Biasutti, et. al. Bulletin ASE/UCS 78/9

[14] W.L. Weeks, Yi Min Diao: Wave propagation characteristics in underground power cable. IEEE Trans. PAS-103 (1984) 10, pp. 2816-2826

[15] J.P. Steiner, P.H. Reynolds, W.L. Weeks: Estimation the location of partial discharges in cables. IEEE Trans. On El. Insulation 27 (1992) 1, pp. 44-59

[16] Partial discharge detection in installed extruded cable systems. Report by CIGRE WG-21-16 (July 2000)

[17] G. Mugala, R. Papazyan, P. Nakov: High frequency characteristics of medium voltage cables using time domain reflectometry techniques. 17th NORD-IS (2001) pp. 211-218

[18] R. Papazyan, R. Eriksson: Calibration for time domain propagation constant measurements on power cables. IEEE Trans. on Instrumentation and Measurement 52 (2003) 2, pp. 415-418

[19] S. Boggs: The case of frequency domain PD testing in the context of distribution cable. IEEE Electrical Insulation Magazine 19 (2003)4, pp. 13-18